ACS OMEGA

Open Access

http://pubs.acs.org/journal/acsodf

Article

Kinetics and Optimization Studies of Controlled 5-Fluorouracil Release from Graphene Oxide Incorporated Vegetable Oil-Based Polyurethane Composite Film

Ebru Kahraman,* Tugba Hayri-Senel, and Gulhayat Nasun-Saygili

Cite This: *ACS Omega* 2024, 9, 47395−47409

Read Online

ACCESS | Metrics & More | Article Recommendations | Supporting Information

ABSTRACT: The current study focuses on investigating the potential of produced graphene oxide (GO)/oil-based polyurethane composite films as a drug carrier for 5-fluorouracil (5-FU). Polyurethane was synthesized starting from blends of castor oil and sunflower oil-based glyceride, followed by GO and 5-FU anticancer drug bearing film production by solution casting. GO/PU composite film samples were characterized by FTIR, TGA and SEM analysis, confirming the PU production and distribution of 5-FU drug at a homogeneous level in GO/PU films. Experimental design studies were carried out to provide insight into the influence of GO incorporation, the amount of loaded drug, and the release medium pH value on 5-FU release behavior. The amount of 5-FU delivered from GO/PU composites displayed a tendency to increase at high GO ratios and high pH values, with the obtained maximum ratio of 91.4%. From release kinetics studies, the pH-sensitive behavior of GO/PU composites was observed following a Higuchi or zero-order kinetic model depending on the GO ratio, indicating a sustained release of the drug. The in vitro cytotoxicity effect of GO/PU film through 5-FU drug release was confirmed against the MCF-7 human breast cancer cell line, while good biocompatibility of the drug-free GO/PU film against the L-929 mouse fibroblast cell line was confirmed via MTT assay test. Overall, the findings support that produced GO/PU composites hold potential for clinical drug delivery applications as a 5-FU drug carrier.

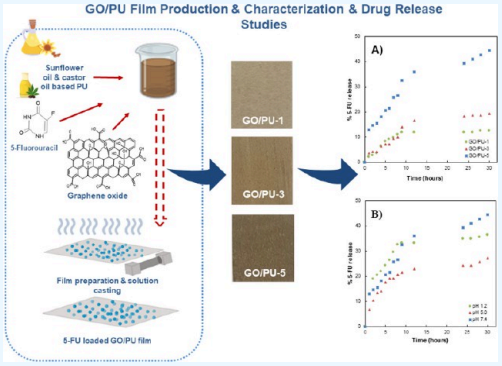

1. INTRODUCTION

Cancer is one of the most fatal morbidities across the world and accounts for the vast majority of mortality among other diseases. An estimated 19.3 million cancer cases have been reported in 2020 and expected to reach up to 28.4 million cases by 2040, featuring the potential dramatic rising of cancer as one of the most compelling threats to human life.[1] Despite the promising medical advances in cancer drug treatments, high toxicity levels arising from sudden and uncontrolled release of drug in the body, affecting healthy tissues together with cancer cells, remains one of the major challenges. Moreover, the interaction of utilized cancer drug with the biological environment can provoke loss of activity and a limited therapeutic effect. Thus, a considerable number of adverse effects including hair loss, fatigue, nausea and skin eruption could occur.[2] In this context, designing drug delivery systems emerges as a crucial alternative for overcoming these limitations by providing controlled administration of the drug.

Graphene oxide is the product of graphene oxidation, and it is the two-dimensional derivative of graphene. The layered morphology of graphene oxide (GO) is decorated with oxygen containing functional groups, which are epoxy and hydroxyl groups on the basal plane, with carboxyl and carbonyl groups at the edges. In recent years, the large surface area and ability to interact with drug molecules through $\pi-\pi$ stacking and hydrogen bonding have rendered GO a promising candidate within drug delivery applications. The existence of oxygen containing functional groups ensures hydrophilic feature enhancing solubility and stability in physiological environment, which in turn contributes substantial biocompatibility.[3,4] On the other hand, utilization of GO in drug delivery applications still necessitates further improvement, due to reports that administration of GO alone might lead to decreasing mammalian cell viability.[5] In order to enhance biocompatibility and prevent possible toxic activity, a wide range of delivery systems have been proposed and investigated for GO functionalization. Accordingly, biomaterials such as gelatin,[6,7] chitosan,[8,9] polysaccharides,[10] polyethylenimine (PEI),[11] polylactic acid (PLA),[12] sodium alginate,[13] carboxymethyl cellulose,[14] β-cyclodextrin (β-CD),[15] pectin,[16] aptamer[17] and polyurethane[18] have been utilized along with GO as a carrier

Received: March 7, 2024
Revised: July 25, 2024
Accepted: July 31, 2024
Published: November 18, 2024

material for various drugs including ibuprofen, doxorubicin, flurbiprofen, 5-fluorouracil, quercetin, curcumin, ceftriaxone, methotrexate, paclitaxel and dexamethasone.

Polyurethane (PU) is an example of the most widely used type of polymers extensively applied in fields as biomedical, textile, automotive, construction, furniture, electronics, aerospace and cosmetics.[19,20] At the molecular level, polyurethanes consist of two fundamental blocks structurally classified as soft parts and hard parts, providing advantageous features including flexibility, abrasion resistance, chemical stability and machinability.[21] The ability to ensure flexibility together with mechanical strength distinguishes polyurethanes in the biomedical field as advantageous materials in particular. To this day, polyurethanes have been widely utilized in catheter tubing, tissue scaffold, heart valve, internal coating of artificial organs, wound dressing, breast implant, bone filler, and drug delivery systems' applications. Above all, their biocompatibility, tunable nature, insolubility in water, and possible pH-sensitive behavior emerges polyurethanes as a promising biomaterial for controlled drug delivery. In recent years, investigations have studied polyurethane as a potential drug carrier structure constituent for the delivery of several drugs such as dexamethasone,[22] olanzapine,[23] curcumin,[24] ciprofloxacin,[25,26] ketoconazole,[27] doxorubicin[28] and 5-Fluorouracil.[29] These designed delivery systems were reported to contribute to the sustained delivery of the aforementioned drugs, unveiling a potential to enhance treatment efficiency. Polyurethane production requires the reaction of isocyanate and alcohol groups, namely polyols, conventionally selected from polyester, polyether, or polycarbonate diols.[30] Apart from the mentioned synthetic petrochemical sources, renewable polyols derived from natural sources also have gained interest due to their lower price, eco-friendly, and processable properties. Concerns over the consumption of petroleum-derived resources have attracted attention for the search for greener alternatives in recent years. In this perspective, vegetable oils including castor oil,[31,32] sun flower oil,[23,33] soybean oil[34,35] and palm oil[36,37] have been researched as polyol sources for PU production.

5-Fluorouracil (5-FU) is one of the most widely administered anticancer agent extensively utilized for cancer treatments such as colon, brain, skin, ovarian, breast, liver, lung and gastric cancer.[38,39] It is an uracil pyrimidine analogue with a fluorine atom at C (Carbon-5) position in the place of hydrogen atom, demonstrating anticancer activity by thymidylate synthase inhibition.[40] Even though 5-FU exhibits remarkable effect in cancer treatments, features as short plasma half-life (8−20 min), toxic adverse effects and nonselectivity to cancer cells limit its therapeutic efficiency.[41] As an approach to overcome these challenges, drug delivery systems have been proposed with the aim of increasing circulation time of 5-FU throughout the body, enhancing the drug content reaching the targeted locations, and consequently minimizing the adverse effects. To the best of our knowledge, a release kinetics and optimization study for the controlled delivery of 5-FU from a GO/oil-based PU composite film have not been studied previously.

The focus of the current study is investigating the potential of produced GO/oil-based PU composite film for the effective delivery of anticancer drug 5-FU while optimizing the controlled delivery of drug. For this purpose, polyurethane was produced starting from blends of castor oil and sunflower oil-based glyceride initially, and PU formation was confirmed by FTIR. Film preparation was completed following GO and 5-FU anticancer drug incorporation, with GO/PU composite films being formed through solution casting. Thereafter, several characterization techniques were employed for the determination of structure, morphology, and anticancer activity of the composites. In order to understand the effect of GO incorporation, 5-FU content, and release medium conditions on 5-FU release behavior, an experimental design study of Box-Behnken design with 3 factors and 3 levels was conducted. Overall, the data are believed to provide useful information for the utilization of GO/oil-based PU composite films as drug delivery systems for biomedical applications.

2. MATERIALS AND METHODS

2.1. Materials. Graphite flakes, 5-FU (≥99%) and castor oil (hydroxyl value: 160−168 mg KOH/g), isophorone diisocyanate (IPDI), and 1,4-butanediol (99%) were purchased from Sigma-Aldrich. Sodium nitrate ($NaNO_3$), sulfuric acid (H_2SO_4 95−98%), hydrogen peroxide (H_2O_2, 30%), calcium hydroxide ($Ca(OH)_2$), glycerol, methanol and hydrochloric acid (HCl, 37%) were purchased from Merck. Dimethylformamide (DMF) was supplied by Carlo Erba. Sunflower oil (Yudum) was purchased from a local market.

2.2. Graphene Oxide (GO) Preparation. GO was produced according to the Hummers Method with minor modifications. Preparation steps were clarified in a previous study.[42]

2.3. Preparation of Sunflower Oil Based Partial Glyceride. As the first step for the oil-based PU production, partial glyceride synthesis was performed from a commercial sunflower oil as reported in a previous study.[43] A 100 g portion of sunflower oil and 8.5 g of glycerin were added to a three-neck flask and stirred at room temperature under a nitrogen atmosphere. After the temperature was raised to 218 °C, 0.1 g of $Ca(OH)_2$ which acted as the reaction catalyst, was added into the flask. Then, the temperature was adjusted to 230 °C and maintained for 1 h. In order to control the completion of the reaction, 1 mL of sample was taken from the reaction medium and mixed with 3 mL of methanol. Depending on the transparency of the obtained mixture, it was confirmed that the reaction was complete. Following the washing and filtering steps, hydroxyl value determination was conducted in order to calculate the amount of isocyanate used in PU production.

2.4. Preparation of Polyurethane (PU). Polyurethane synthesis was carried out by the reaction of diisocyanate with a mixture of partial glyceride/castor oil (CO) as a hydroxyl source. Depending on the reports associating castor oil with improved flexibility, with the use of castor oil along with glyceride as a polyol, it was aimed to provide flexibility to obtained GO/PU films.[44,45] In addition, it was reported that sunflower oil-based PU film tended to leave residues on the applied surface after being peeled off, and CO incorporation could improve such behavior.[46] Hence, CO addition was also preferred to ensure easy removal of GO/PU films from an applied polypropylene sheet surface. In a three-neck flask, 5 g of glyceride/CO mixture (glyceride/CO = 1 (w/w)) was added and stirred until a homogeneous mixture was obtained. After 0.44 g of 1,4-butanediol was added as a chain extender, 4.36 g of IPDI was also added dropwise according to the stoichiometric ratio of OH/NCO = 1. Meanwhile, the mixture was kept under moderate cooling in order to prevent a premature start of the reaction. Then, the temperature was raised to 40 °C and maintained for 30 min, followed by constant stirring at 90 °C for 1.5 h in order for the

https://doi.org/10.1021/acsomega.4c02247
ACS Omega 2024, 9, 47395−47409

polymerization reaction to be completed. At the end of 1.5 h, the final product was left to cool at room temperature.[43]

2.5. Preparation of 5-FU Loaded Graphene Oxide/Polyurethane Composite (GO/PU). GO/PU composites including 1, 3, and 5 (wt %) ratio of GO were synthesized by solution casting method and referred to as GO/PU-1, GO/PU-3 and GO/PU-5 (Scheme 1). First, GO was dispersed in DMF and ultrasonicated for 30 min. Upon sonication, 5-FU was added to the GO/DMF mixture and stirred for another 30 min. Then, obtained GO/DMF/5-FU mixture was added dropwise in 1 g of synthesized PU followed by stirring for about an hour until homogeneity was achieved. The obtained mixture was left at room temperature for 1 day for evaporation of the solvent. This procedure was repeated for all determined GO and 5-FU amounts presented in 2.8 Experimental Design. After solvent evaporation, the resultant GO/PU composite was coated on a polypropylene sheet surface with a film applicator (60 μm thickness) and dried at room temperature for 2 days. For characterization purposes, composites were also produced without 5-FU incorporation. Images of obtained GO/PU composites with increasing GO amounts are given in Figure 1.

Scheme 1. Preparation Steps of 5-FU Incorporated GO/PU Composites

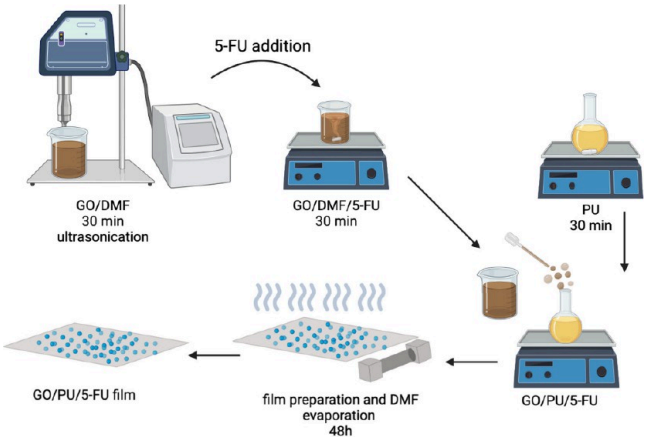

2.6. In Vitro Drug Release of 5-FU from GO/PU Composite. The following procedure was employed for studying the drug release of 5-FU from GO/PU. First, 2 × 2 cm of produced GO/PU films were cut out and placed into a dialysis tubing membrane (Sigma, 14 kDa) involving 5 mL of buffer solution. Then, dialysis tubing was transferred to a beaker containing 100 of the buffer solution. A release study was carried out in a shaking water bath operated at 37 °C and 120 rpm. Samples were withdrawn from the release medium at specific time intervals, and the absorbance values were measured via ultraviolet−visible (UV−vis) spectrophotometer (Hach DR6000) at 266 nm. Obtained absorbance data was used for the calculation of the released 5-FU amount. This procedure was repeated for varying pH values of the release medium and varying GO/PU composites.

2.7. Drug Release Kinetics. The data derived from release studies were studied by applying five distinct mathematical models including zero-order, first-order, Korsmeyer−Peppas, Higuchi and Hixson−Crowell models to provide insight into release kinetics of 5-FU from the composites. Calculated correlation coefficients (R^2) were examined and the kinetic model with the R^2 closest to 1 was accepted as the best fitting model. Zero-order kinetic model equation is expressed by eq 1 as follows:

$$C_t = C_0 + K_0 t \tag{1}$$

here t represents time, C_t is the amount of released drug during the time t, C_0 is the initial drug concentration which is generally equal to 0 and K_0 is the zero-order model constant. First-order kinetic model equation is proposed as in eq 2:

$$\log Q_1 = \log Q_0 + \frac{K_1 t}{2.303} \tag{2}$$

with Q_1 standing for the amount of released drug during the time t, Q_0 for the initial amount of drug dissolved and K_1 for the first-order model constant.[47] eq 3 describes the Korsmeyer−Peppas model equation as

$$\log(M_i/M_\infty) = \log K + n\log t \tag{3}$$

in which M_∞ is the drug amount at equilibrium, M_i is the amount of released drug during the time t, K is the constant and n is the release exponent.[48] The n value close to 0.5 can be interpreted as Fickian diffusion and n = 0.5 as Fickian model (Case I), whereas n = 1 is a sign of non-Fickian (Case II) model. A n value of $0.5 < n < 1$ refers to a non-Fickian or anomalous transport, while $n > 1$ suggest the system follows super case II transport. Higuchi kinetic model is presented by eq 4 as follows:

$$Q = K_H \sqrt{t} \tag{4}$$

where Q defines the amount of released drug on time t and K_H the Higuchi release constant.[49] Hixson−Crowell kinetic model is represented in eq 5 as

$$\sqrt[1/3]{W_0} = \sqrt[1/3]{W_i} + K_{HC} t \tag{5}$$

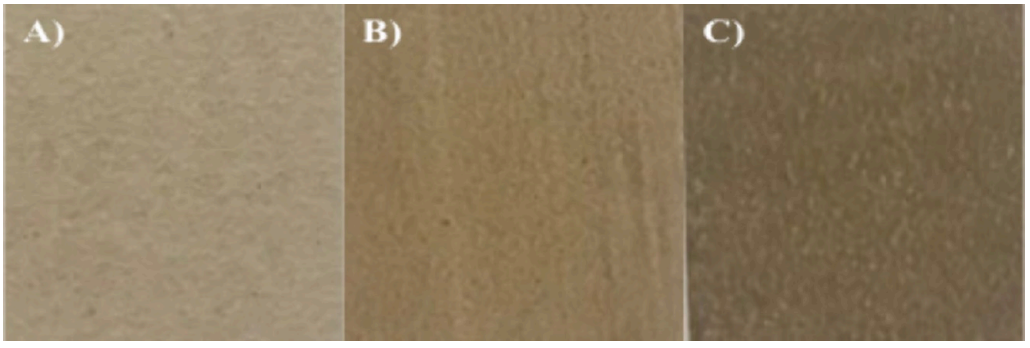

Figure 1. Images of GO/PU films with different GO amounts; A) GO/PU-1, B) GO/PU-3, and C) GO/PU-5.

https://doi.org/10.1021/acsomega.4c02247
ACS Omega 2024, 9, 47395−47409

where W_0 stands for the initial amount of drug in the delivery system, W_i for the amount of drug remained in the delivery system at time t and K_{HC} for the constant of incorporation.[50,51]

2.8. Experimental Design. Box-Behnken design with 3 factors and 3 levels was employed to optimize the 5-FU release from GO/PU composites as presented in Table 1. GO amount

Table 1. Designated Levels Used in the Box-Behnken Design with Independent and Dependent Variables

		Levels		
Factors/Independent variables	Symbol	Low (−1)	Medium (0)	High (1)
GO amount ((w/w)%)	X_1	1	3	5
Initial 5-FU concentration (mg/mL)	X_2	5	10	15
pH value of release medium	X_3	2	6	10
Dependent variable				
Y_1 = Released amount of 5-FU ((w/w)%)				

((w/w)%), initial 5-FU concentration (mg/mL), and pH value of release medium were selected as the independent variables, and their influence were investigated at three different levels (low (−1), medium (0), high (1)). The response of the designed experiment was determined as released amount of 5-FU ((w/w)%) (Y_1), which was the dependent variable. The design formula displayed a total of 15 experimental runs with 3 center points. Obtained data was analyzed, a quadratic second-order polynomial was fitted, and contour plots were created via Minitab 21 Software. Significance of the selected independent variables were examined accounting for analysis of variance (ANOVA, p-value <0.05) and compatibleness of the model was invesitgated by using R^2 and adjusted R^2 values. By analyzing the contour plots, individual and bilateral interactions of the variables were demonstrated.

2.9. Characterization. The interaction between graphene oxide, polyurethane and 5-FU were analyzed by FT-IR spectrophotometer (Bruker) in the range of 650 cm^{-1} to 4000 cm^{-1}. Thermogravimetric analysis (TGA) was carried out by PerkinElmer Diamond TG/DTA under nitrogen atmosphere at a heating rate of 10 °C/min from 25 to 550 °C. The surface morphologies, elemental compositions, and mappings of GO/PU composites were obtained from scanning electron microscope (SEM, Zeiss EVO LS 10) equipped with EDAX operated at 10 kV. In vitro cytotoxicity of produced GO/PU and 5-FU incorporated GO/PU films were assessed by MTT assay test against L-929 mouse fibroblast cell line and MCF-7 human breast cancer cell line, respectively, using extraction method.

3. RESULTS AND DISCUSSION

3.1. FTIR Analysis. FTIR spectra of PU, GO/PU-1, GO/PU-3 and GO/PU-5 samples were presented in Figure 2. The absence of the characteristic isocyanate peak (-NCO) in lean PU spectra normally observed around 2270 cm^{-1} confirmed that -NCO groups completely reacted with O−H groups.[52] Additionally, the peak that emerged at 3350 cm^{-1} can be assigned to the N−H stretching of urethane and urea groups. While the peaks at 1696 cm^{-1} indicated the presence of carbonyl groups of urethane and urea groups, the peaks at 2924 cm^{-1} were due to C−H stretching vibration of alkane.[53] Figure 3 represented the FTIR spectra of 5-FU loaded GO/PU-1/5-FU, GO/PU-3/5-FU and GO/PU-5/5-FU composites. Comparing the 5-FU loaded and unloaded composites, significant characteristic peaks of 5-FU were not observed in the drug-loaded composites. This might be explained by the fact that 5-FU molecules were found embedded in the PU matrix, which prevented the detection of drug's characteristic wavelengths from the surface.

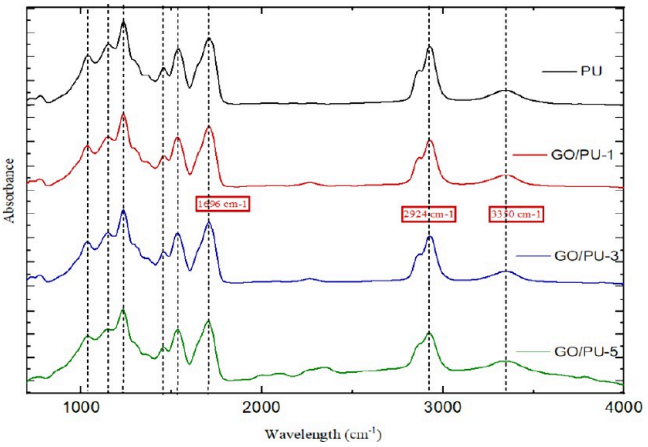

Figure 2. FTIR spectra of PU, GO/PU-1, GO/PU-3 and GO/PU-5 composites.

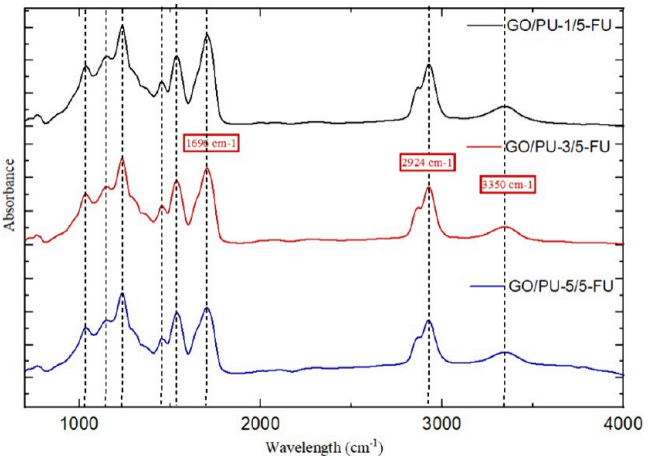

Figure 3. FTIR spectra of GO/PU-1/5-FU, GO/PU-3/5-FU ve GO/PU-5/5-FU composites.

3.2. TGA Analysis. The thermal stabilities of PU and GO/PU composites were examined as observed in Figure 4. The thermal decomposition took place in two main steps for all samples. The initial mass loss around 300 °C can be attributed to the breakage of urethane bonds. Whereas the second significant mass loss loss around 450 °C indicated the degradation of soft segments. After 500 °C temperature was reached, PU and GO/PU-5 samples were completely consumed while the remaining mass of composites with 1 and 3% GO content were obtained approximately 4−5%. In addition, a small drop in degradation temperature was observed with the incorporation of GO. This could be explained by graphene oxide acting as a heat source because of its good thermal stability and conductivity, therefore accelerating the thermal degradation.[54] The two-step degradation of the samples could also be detected in DTG analysis given in Figure 5. The increase in the area under the DTG curve implies higher mass loss during thermal treatment. Therefore, the decrease in the areas under DTG curves around

https://doi.org/10.1021/acsomega.4c02247
ACS Omega 2024, 9, 47395−47409

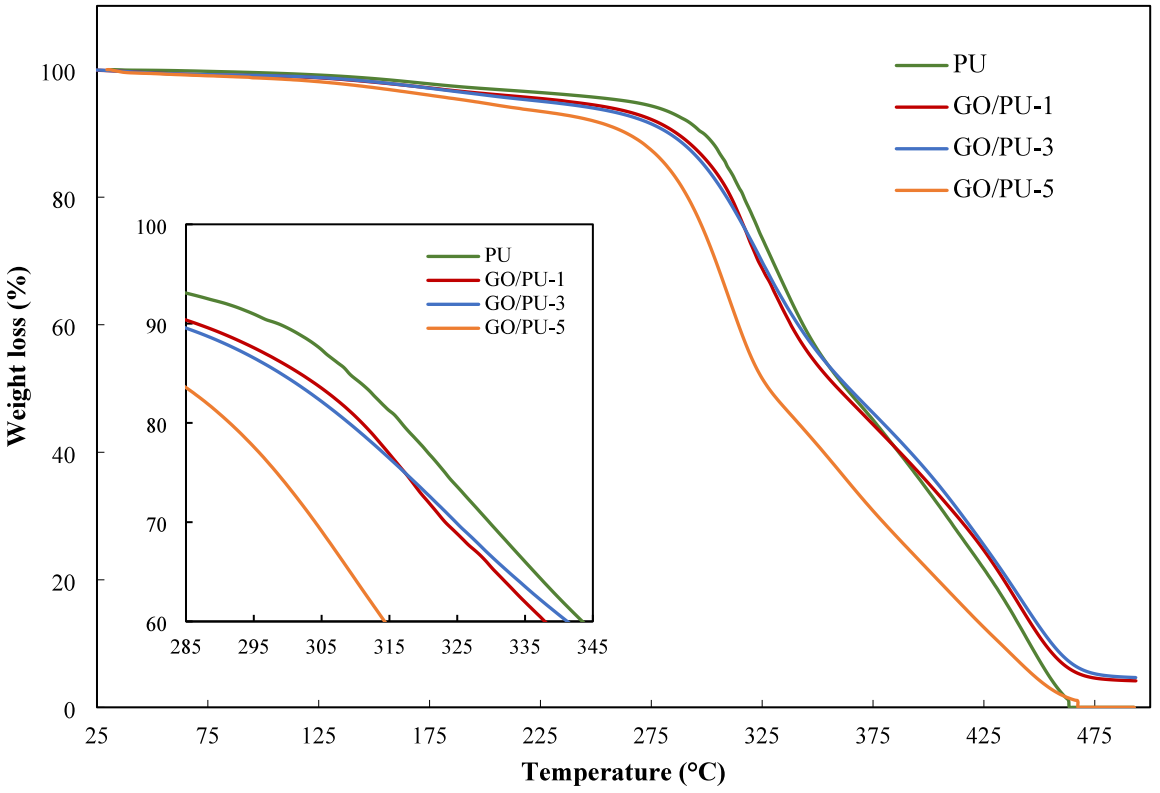

Figure 4. TGA curves of PU, GO/PU-1, GO/PU-3 and GO/PU-5.

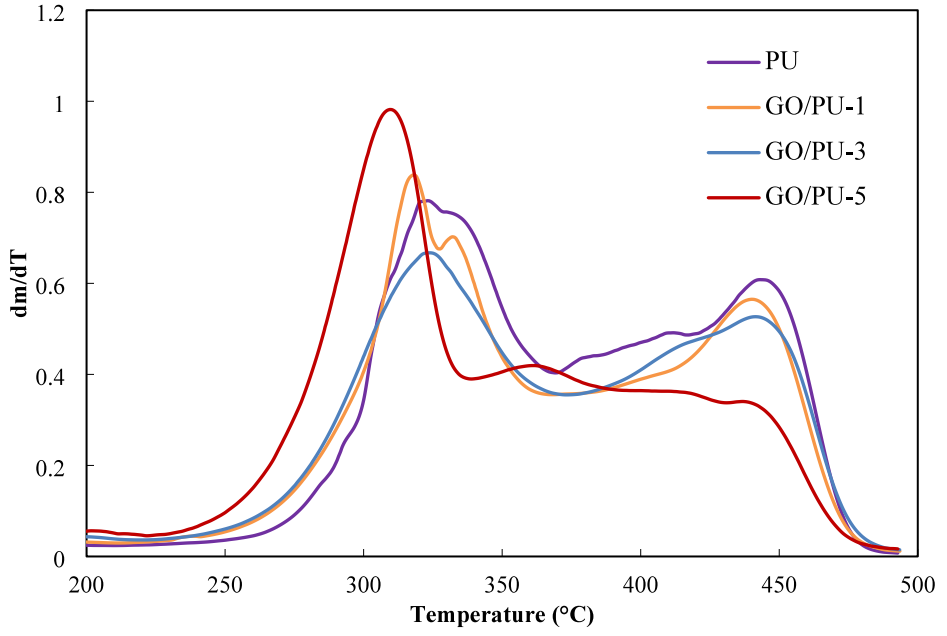

Figure 5. DTG curves of PU, GO/PU-1, GO/PU-3 and GO/PU-5.

450 °C with increasing GO content was a sign of thermal stability improvement effect of GO.[55] In contrast, the highest area under the DTG curves around 300 °C belonged to the composite with the highest GO content. This could be also attributed to the graphene oxide's heat source effect accelerating the degradation, which was explained above in Figure 4.

3.3. SEM Analysis. The microscopic structure of GO/PU composites were visualized via SEM imaging as presented in Figure 6. The wrinkled and sheet like surface of the GO were covered with PU, and small hole structures were detected possibly due to solvent evaporation step during production. With increasing GO content, a rougher surface was observed in comparison with those of lower GO containing composites. The elemental mapping of 5-FU loaded composites confirmed the homogeneous distribution of C, N, O and F atoms (Figure 7). Also, the overall appearance and similar ratio of F atoms

https://doi.org/10.1021/acsomega.4c02247
ACS Omega 2024, 9, 47395−47409

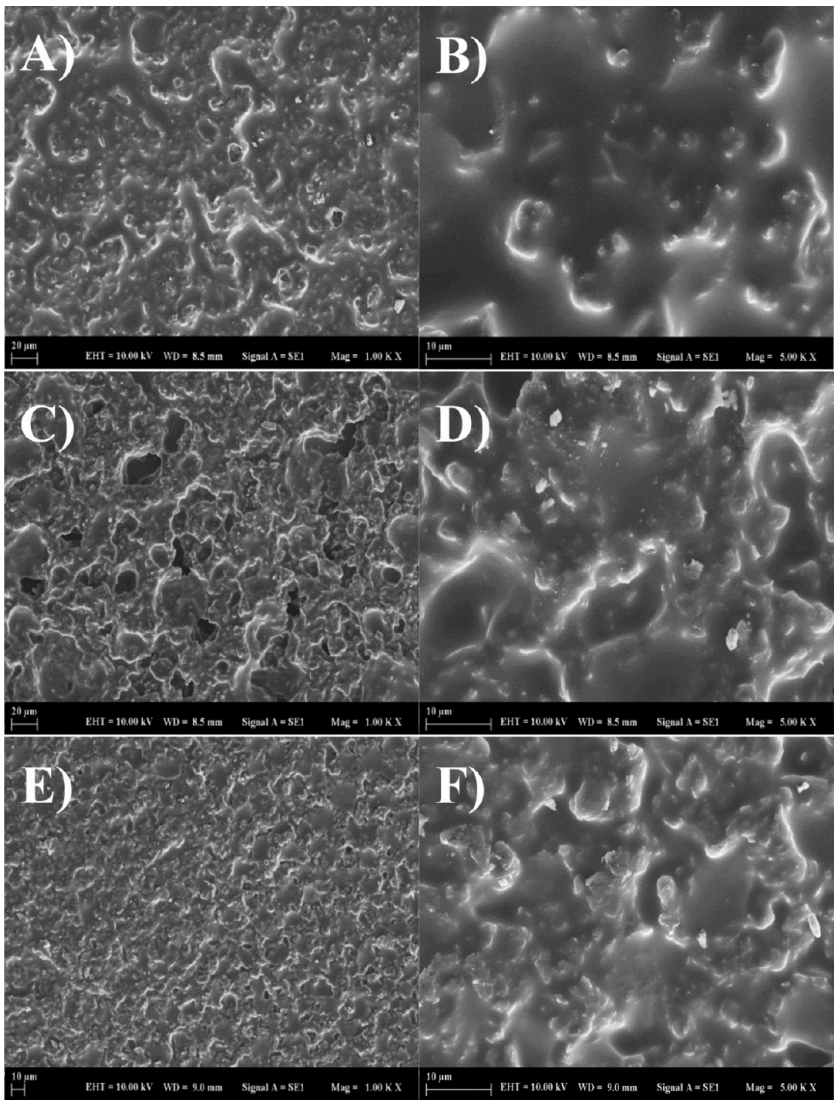

Figure 6. SEM images of GO/PU-1 (A, B), GO/PU-3 (C, D), and GO/PU-5 (E, F) composites.

approved that the 5-FU drug distributed homogeneously in GO/PU films.

3.4. Experimental Design and Optimization Studies. The findings of Box-Behnken design experiments are summarized in Table 2 including experimental and predicted values. The maximum and minimum release percentages of 5-FU was obtained as 91.36% (F9) and 0.84% (F14) respectively. The ANOVA test results are given in Table 3. Following the elimination of insignificant terms from the quadratic model (p-value <0.05), the mathematical expression obtained for the 5-FU release from GO/PU was given in eq 6 as follows:

$$Y_1 = 13.43 + 17.31X_1 - 16.40X_2 + 19.02X_3 + 9.60X_1^2 + 17.02X_2^2 - 8.94X_1X_2 + 14.53X_1X_3 - 24.43X_2X_3 \quad (6)$$

According to design experiment data, R^2 and adjusted R^2 values were found as 99.38% and 98.54% respectively. As observed from the Table 3, the p value of the model was below 0.05 together with a p value for lack of fit higher than 0.05 (F = 5.61, p = 0.157), confirming that the model displayed an acceptable significance level.

3.4.1. Effect of Independent Variables on 5-FU Release by Assessing Contour Plots. The impact of independent variables on 5-FU release from GO/PU was shown by three-dimensional surface and contour plots comparatively in Figure 8. As observed in Figure 8A and 8B, the maximum percentage of drug release was obtained for a high GO amount and low 5-FU initial concentration. While the increasing GO amount at constant initial 5-FU concentration increased the release percentage, the increase in the 5-FU initial concentration at a constant amount of GO significantly reduced the release percentage. As seen in Figure 8C and 8D, the increment in the amount of GO at low release medium pH values did not make a significant difference, whereas it caused an increment in the drug release percentage at high release medium pH values. Similarly, an increase in the release medium pH value at constant GO values led to an increase in the release percentage. Considering Figure 8E and 8F, the maximum release percentage was obtained with the increase in the release medium pH and the decrease in the initial concentration of 5-FU. Depending on both model equation and plots, it can be concluded that the release medium pH value X_3(C) is the most dominant factor, with all three factors being effective on the release percentage. This was also affirmed by the fact that the

https://doi.org/10.1021/acsomega.4c02247
ACS Omega 2024, 9, 47395−47409

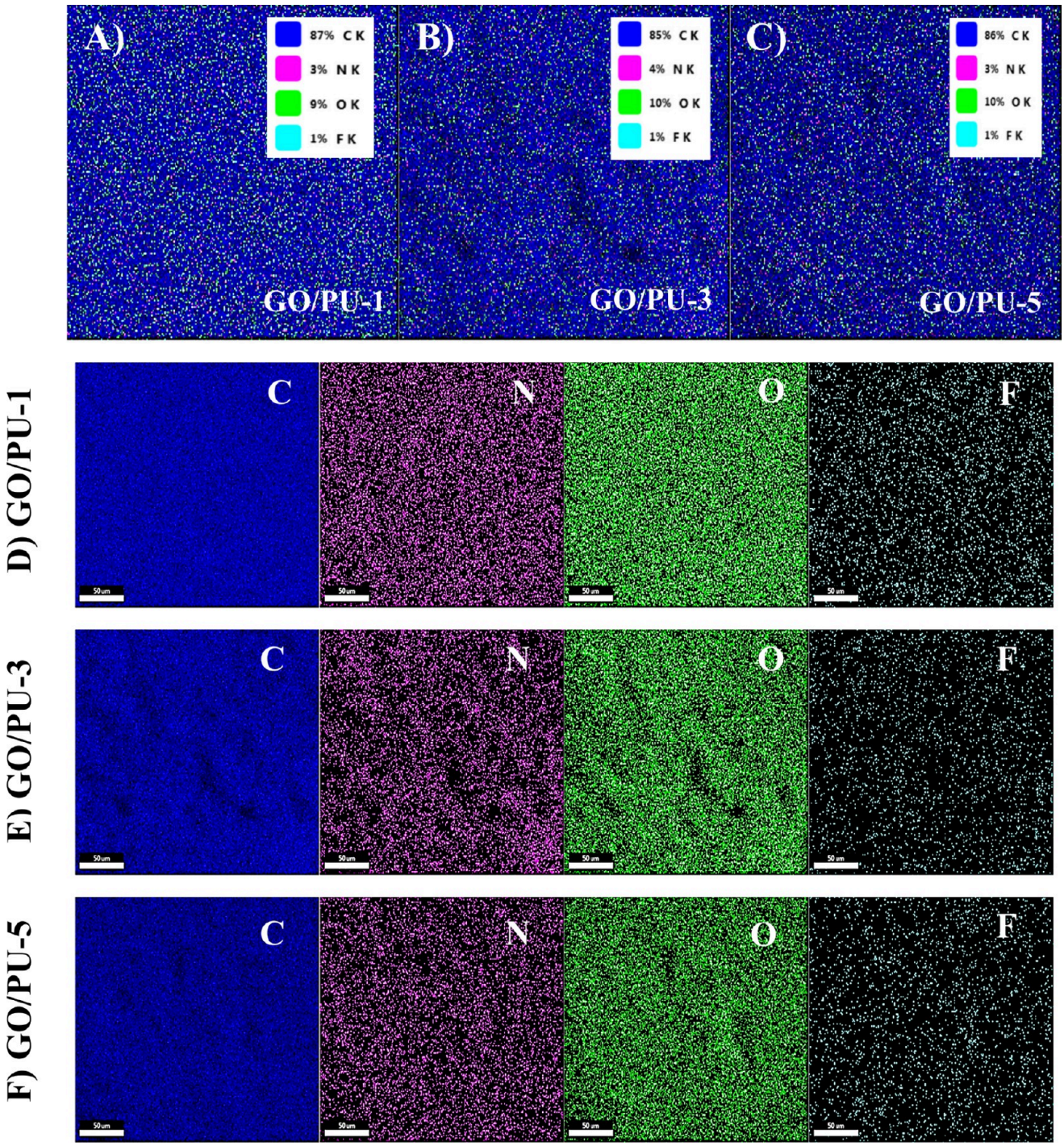

Figure 7. Elemental mapping of 5-FU loaded GO/PU-1 (A-D), GO/PU-3 (B-E) and GO/PU-5 (C−F) composites.

coefficient of the X_3 term in the model equation was higher than the coefficients of the X_1 and X_2 terms. Obtaining p values as 0.000 (<0.05) for all three terms validated the selected factors and level ranges created a significant difference on the 5-FU release percentage. Similarly, the terms X_1^2 and X_2^2 were left in the model equation due to high significance levels (X_1^2: p = 0.002, X_2^2: p = 0.000), while the X_3^2 term was removed because of a p value larger than 0.05 (X_3^2: p = 0.723). In terms of bilateral interactions, the p values of all three terms X_1X_2, X_1X_3 and X_2X_3 were obtained as <0.05 (X_1X_2: p = 0.003, X_1X_3: p = 0.000, X_2X_3: p = 0.000) and owing to the high levels of significance, the model terms were left in the eq (eq 6). Finally, the experimental and predicted values derived from the model equation are given comparatively in Figure 8G.

In summary, overall data demonstrate that the drug release percentage increases significantly at high GO amount, high release medium pH levels, and low 5-FU initial concentrations. Also, the singular and bilateral interactions of all three factors have a significant effect on the drug release rate. The fact that the release medium pH value stands out as an effective factor indicates that the produced films perform pH-sensitive release. It is a known fact that polyurethane materials can display pH-sensitive behavior, allowing them to be preferred in biomedical and drug delivery system applications. One of the reasons that

https://doi.org/10.1021/acsomega.4c02247
ACS Omega 2024, 9, 47395−47409

Table 2. Box-Behnken Experimental Design Points and Responses with Their Experimental and Predicted Values[a]

Runs	Independent variables			Dependent variables	
	X_1	X_2	X_3	Y_1	
				Experimental	Predicted
F1	1	10	2	1.35	1.23
F2	3	10	6	10.91	13.43
F3	3	10	6	13.99	13.43
F4	1	5	6	32.97	30.20
F5	1	15	6	15.87	15.28
F6	5	5	6	81.41	82.70
F7	5	15	6	28.55	32.02
F8	3	15	10	11.91	8.64
F9	3	5	10	91.36	90.30
F10	3	15	2	19.09	19.46
F11	3	10	6	13.99	13.43
F12	5	10	2	10.98	6.79
F13	1	10	10	6.71	10.21
F14	3	5	2	0.84	3.40
F15	5	10	10	74.46	73.89

[a]$\mathbf{X_1}$ = GO amount ((w/w)%); $\mathbf{X_2}$ = Initial 5-FU concentration (mg/mL); $\mathbf{X_3}$ = pH value of release medium; $\mathbf{Y_1}$ = Released amount of 5-FU ((w/w)%).

Table 3. ANOVA Results for the Box-Behnken Experimental Design[a]

Source	DF	Adj SS	Adj MS	*F*-Value	*P*-Value
Model	8	12333.0	1541.63	119.44	0.000
Linear	3	7443.9	2481.30	192.25	0.000
$\mathbf{X_1}$	1	2398.1	2398.07	185.80	0.000
$\mathbf{X_2}$	1	2150.5	2150.52	166.62	0.000
$\mathbf{X_3}$	1	2895.3	2895.32	224.32	0.000
Square	2	1338.3	669.15	51.84	0.000
$\mathbf{X_1}$* $\mathbf{X_1}$	1	342.1	342.14	26.51	0.002
$\mathbf{X_2}$* $\mathbf{X_2}$	1	1076.0	1076.01	83.37	0.000
2-Way Interaction	3	3550.8	1183.61	91.70	0.000
$\mathbf{X_1}$*$\mathbf{X_2}$	1	319.9	319.88	24.78	0.003
$\mathbf{X_1}$*$\mathbf{X_3}$	1	844.5	844.54	65.43	0.000
$\mathbf{X_2}$* $\mathbf{X_3}$	1	2386.4	2386.41	184.89	0.000
Error	6	77.4	12.91		
Lack-of-Fit	4	71.1	17.78	5.61	0.157
Pure Error	2	6.3	3.17		
Total	14	12410.5			

[a]$\mathbf{X_1}$ = GO amount ((w/w)%); $\mathbf{X_2}$ = Initial 5-FU concentration (mg/mL); $\mathbf{X_3}$ = pH value of release medium; $\mathbf{Y_1}$ = Released amount of 5-FU ((w/w)%).

provides polymers with pH-sensitive characteristics is containing ionizable acidic or basic functional groups. In environments with different pH values, ionizable functional groups can become protonated or lose protons. Polymers with acidic functional groups such as carboxylic acid, sulfonic acid, or methacrylic acid dissolve in a high pH environment and lose protons. This causes high charge density due to electrical repulsion between the chains and the absorption of water. Absorption of water results in swelling of the polymer and the release of the drug content. In a low pH environment, polymers containing basic functional groups swell as a result of the protonation of these groups and show pH sensitive properties.[56] In the case of produced GO/PU composite films, the maximum percentage of released drug at low pH was around 19%, while this value reached up to 91% at high pH values (Table 2). This can be associated with the carboxyl groups in the GO structure. Carboxyl groups are among the ionizable acid functional groups. Accordingly, it can be concluded that the films swell and the drug is released effectively owing to the electrostatic repulsion induced by the proton loss of the carboxyl groups in the composite's structure in the pH 10 environment. In addition, the surface charge alteration of 5-FU molecules depending on pH value might have influenced the release pattern. 5-FU is reportedly known to display a pK_a value in the range of 7.6 and 8.05.[57,58] The presence of two potential deprotonation sites on the amide N1and N3 nitrogen allows 5-FU to be found in two anionic forms above its pK_a value.[59] Therefore, possible ionization of 5-FU molecules at pH 10 condition might enhance the electrostatic repulsion through composite matrix leading to higher release ratios. Also, a higher percentage of released drug with increasing GO% ratio can be explained by the increment in the absorbed amount of water and swelling, due to the increased number of carboxyl groups in the composite's structure.

3.5. Drug Release Kinetics of 5-FU from GO/PU. The kinetics of 5-FU drug release from GO/PU composite was studied at three different pH values including 1.2, 5.0, and 7.4 simulating the pH of gastric, tumor and physiological environment, respectively.[60−63] As 5-FU release percentages have a tendency to increase with higher GO content according to the experimental design data, the composite with the highest GO content (GO/PU-5) was selected. Also, the effect of the GO content was studied at pH 7.4. The release percentages of 5-FU drug in proportion to total incorporated drug during composite production were presented in Figure 9. Release of 5-FU from GO/PU samples completed upon 30 h with an observed significant release amount in first 9 h, demonstrating an almost biphasic release behavior. As the major part of the release occurred within 9 h, release kinetic profiles were decided to be generated in this time region. The release kinetics were evaluated by five distinct kinetic models including zero-order, first-order, Korsmeyer−Peppas, Higuchi and Hixson−Crowell model, which are shown in Figures S1, S2, S3, S4 and S5. Release percentages of 5-FU drug were calculated in proportion to the total released drug from the composites. Calculated release kinetics parameters were presented in Table 4 and Table 5.

3.5.1. Effect of pH. The R^2 values obtained from the mathematical models (Table 4) revealed that Higuchi kinetic model was emerged as the best fit at all pH values with the highest R^2 values of 0.9830, 0.9891, and 0.9532 at pH 1.2, 5.0, and 7.4 respectively. Following Higuchi model release behavior could be interpreted as the release occurs through diffusion and dissolution of the drug with a release in direct proportion to the square root of time.[64] Drug release from the polymer matrix via diffusion involves the steps of water entering through polymer matrix, dissolving the drug, and followed by diffusion of drug out of the matrix. Similar release behavior following the Higuchi kinetic model for different PU based drug carriers was also reported in the literature.[24,65]

The initial burst of 5-FU from the composite slightly differed with the effect of the release medium pH, as observed from Figure 10. The release percentage of 5-FU from the GO/PU-5 composite at pH 1.2, 5.0, and 7.4 were obtained as 52.0%, 38.0% and 32.9%, respectively, at the end of the second hour. With increasing pH, the initial burst release converted into a

https://doi.org/10.1021/acsomega.4c02247
ACS Omega 2024, 9, 47395−47409

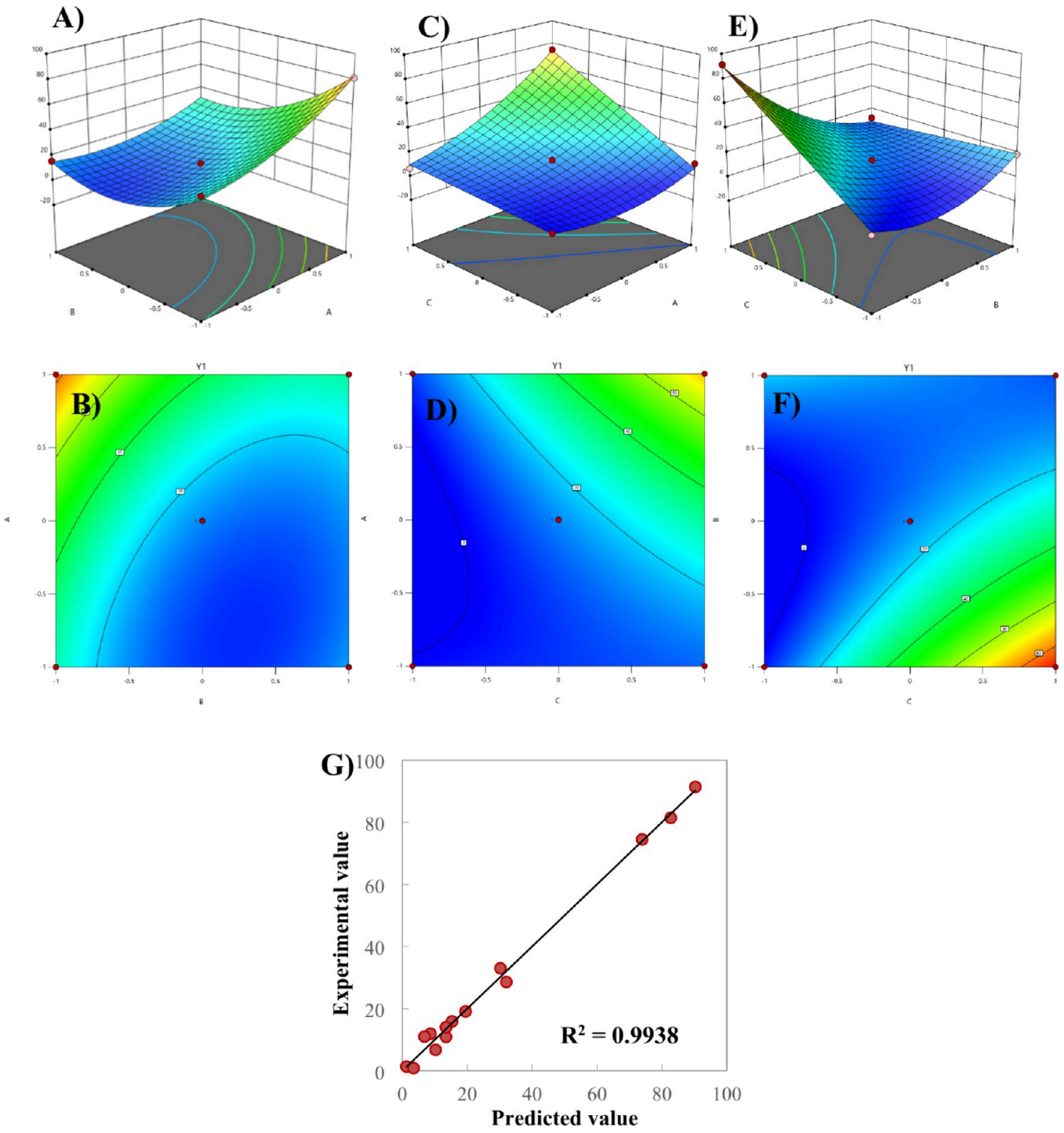

Figure 8. Three dimensional surface and contour plots of 5-FU release parameters showing the effect of independent variables (A: GO amount ((w/w)%), B: Initial 5-FU concentration (mg/mL); C: pH value of release medium, C8: Released amount of 5-FU ((w/w)%)), A-B) GO amount ((w/w)%) vs initial 5-FU concentration (mg/mL), C-D) GO amount ((w/w)%) vs pH value of release medium, E-F) initial 5-FU concentration vs pH value of release medium, G) experimental values vs predicted values of the released amount of 5-FU.

lower trend, approaching a steadier release. The slight increase in the initial burst values at acidic pH could be related to the enhanced solubility of graphene oxide in acidic mediums. The enhanced solubility of GO might have allowed the increase of diffusion coefficient of 5-FU, resulting in faster release from the composite matrix.[66] In order to have a better understanding of the release mechanisms, the *n* values evaluated from the Korsmeyer−Peppas model were examined. The *n* values at pH 1.2 (0.4161) and pH 7.4 (0.4009) conditions implied that diffusion is the main mechanism controlling the release. However, at pH 5.0 condition, the *n* value above 0.5 (0.5305) signified disordered transport state (non-Fickian) and different mechanisms might have affected the release kinetics along with diffusion. Overall data suggested that 5-FU release from GO/PU composites was a function of pH, indicating pH sensitive release behavior.

3.5.2. Effect of GO Ratio. The release profiles of GO/PU-1 and GO/PU-3 composites displayed initial burst release rates

https://doi.org/10.1021/acsomega.4c02247
ACS Omega 2024, 9, 47395−47409

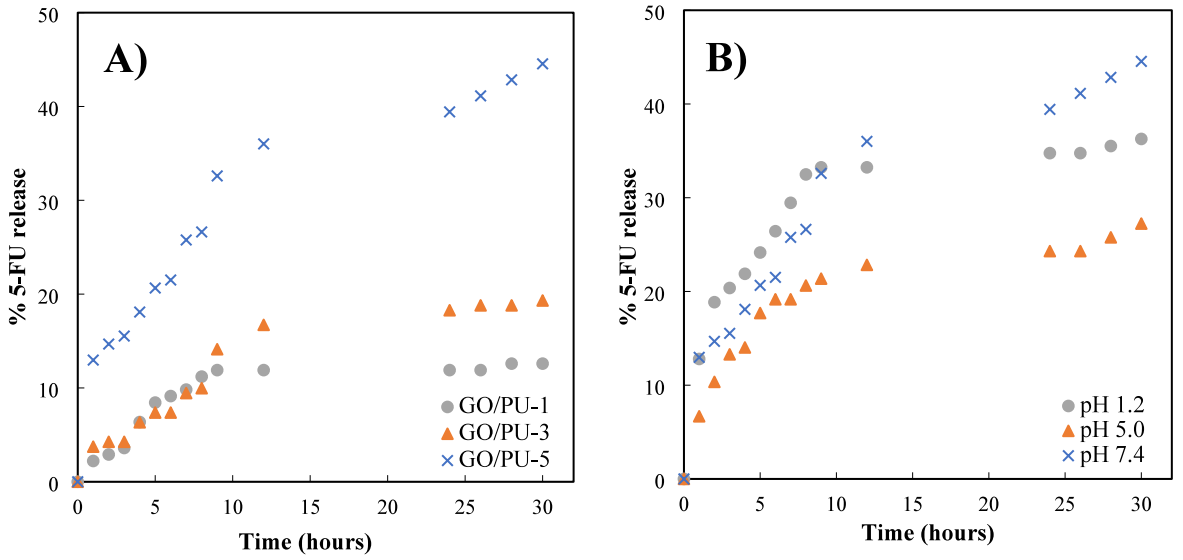

Figure 9. Release profiles of 5-FU from A) GO/PU-1, GO/PU-3 and GO/PU-5 (temperature: 37 °C, pH: 7.4) and B) GO/PU-5 at pH 1.2, 5.0, and 7.4 (temperature: 37 °C) in proportion to total incorporated drug.

Table 4. Release Kinetic Parameters of 5-FU Loaded GO/PU-5 Composite at pH 1.2, 5.0, and 7.4

Model	Zero-order		First-order		Korsmeyer−Peppas		Higuchi		Hixson−Crowell	
pH	K_0	R^2	K_1	R^2	n	R^2	K_H	R^2	K_{HC}	R^2
1.2	8.5282	0.8798	0.2510	0.9513	0.4161	0.9762	31.047	0.9830	0.2603	0.9634
5.0	7.9038	0.8937	0.1660	0.9776	0.5305	0.9832	27.085	0.9891	0.1974	0.9588
7.4	6.3202	0.9015	0.1145	0.9170	0.4009	0.8889	21.780	0.9532	0.1438	0.9251

Table 5. Release Kinetic Parameters of 5-FU Loaded GO/PU-1, GO/PU-3 and GO/PU-5 Composites at pH 7.4

Model	Zero-order		First-order		Korsmeyer−Peppas		Higuchi		Hixson−Crowell	
Composite	K_0	R^2	K_1	R^2	n	R^2	K_H	R^2	K_{HC}	R^2
GO/PU-1	10.748	0.9750	0.3015	0.9224	0.8526	0.9510	28.220	0.8912	0.3145	0.9710
GO/PU-3	6.4964	0.9282	0.1108	0.8405	0.5754	0.8547	18.396	0.8649	0.1419	0.8808
GO/PU-5	6.3202	0.9015	0.1145	0.9170	0.4009	0.8889	21.780	0.9532	0.1438	0.9251

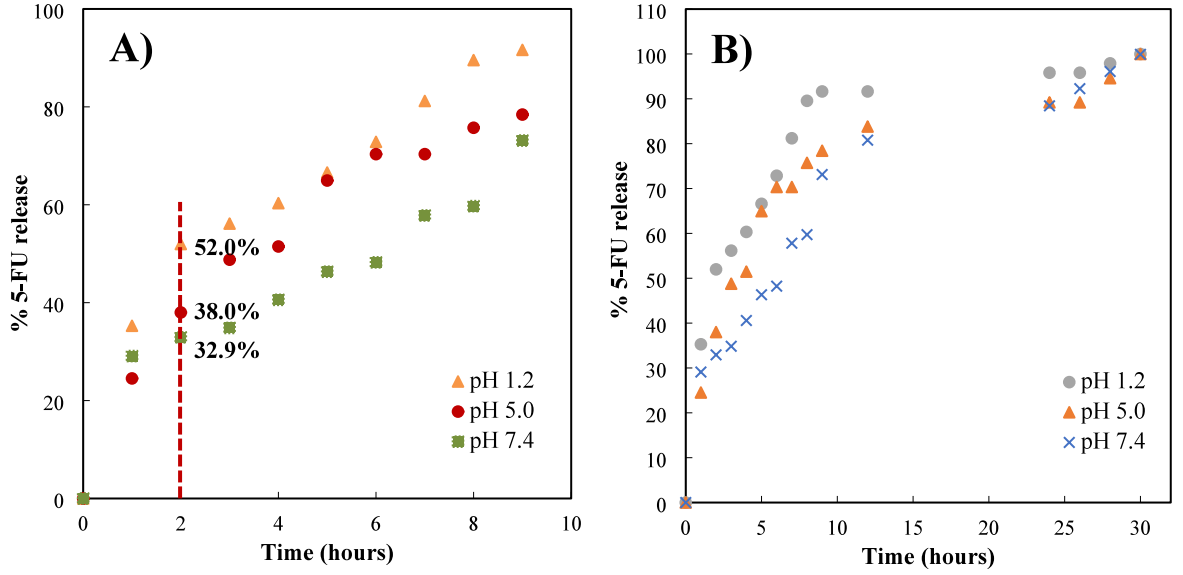

Figure 10. Release profiles of 5-FU from GO/PU-5 at pH 1.2, 5.0, and 7.4 A) in initial 9 h, B) after 30 h (temperature: 37 °C) in proportion to total released drug.

https://doi.org/10.1021/acsomega.4c02247
ACS Omega 2024, 9, 47395−47409

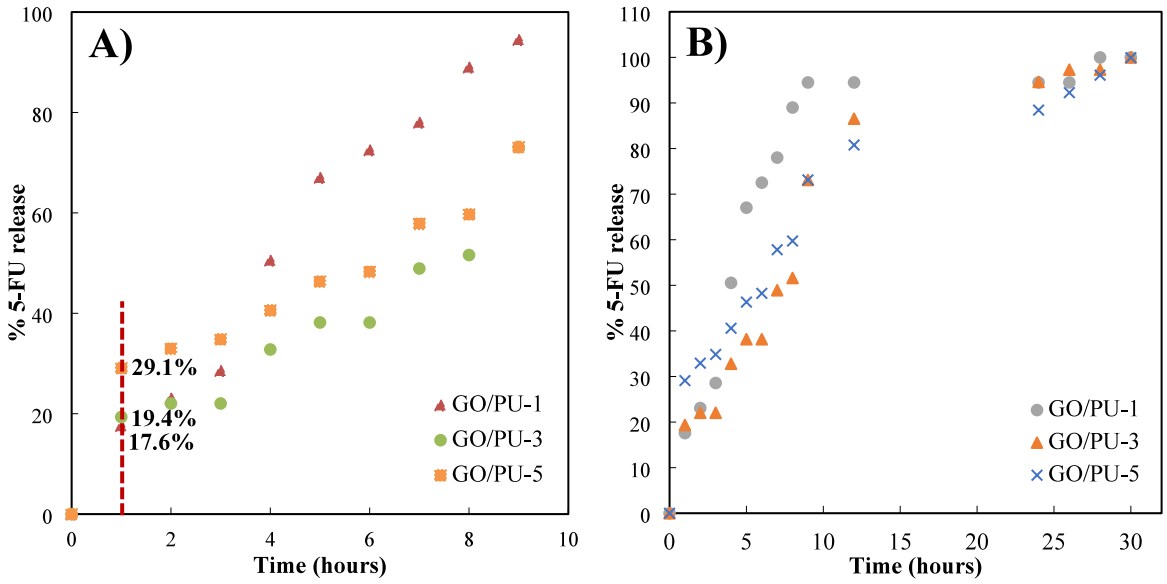

Figure 11. Release profiles of 5-FU from GO/PU-1, GO/PU-3 and GO/PU-5 in A) initial 9 h and B) after 30 h (temperature: 37 °C, pH: 7.4) in proportion to total released drug.

Table 6. Summary of Drug Release Studies of PU Based Drug Carriers

Material	Drug	Release percentage	Kinetic model	refs
PU microsphere	Dexamethasone	20−60% (10 days)	-	22
PU nanoparticle	Olanzapine	82% 168 h	Higuchi	23
PU/dextran membrane	Curcumin	8−15% (500 min)	Higuchi	24
PU films	Ciprofloxacin	40−70% (10 days)	-	25
PU/urea elastomer film	Ciprofloxacin	20−55% (90 days)	-	26
Collagen/PU composite reinforced with cellulose	Ketoconazole	300−1000 ppm (250 min)	Korsmeyer−Peppas	27
PU based hydrogel	5-Fluorouracil	40−60% (3 days)	-	29
Waterborne poly(urethane-urea)s	Ketoconazole	Above 80% (8 h)	Higuchi First-order	65
Lignin based PU	Ammonium sulfate	5−30% (31 days)	Korsmeyer−Peppas	69
Thermoplastic PU based intravaginal ring	Lactic acid or metronidazole	60−100% for lactic acid (28 days) 50−100% for metronidazole (7 days)	-	70
PU films	Cefazedone	5−55% (48 h)	-	71
GO/PU composite film	5-Fluorouracil	25−45% (30 h)	Higuchi Zero-order	This study

of 17.6% and 19.4% after 1 h, respectively (Figure 11). Comparing with GO/PU-5, which released 29.1% of the loaded 5-FU in 1 h, revealed that composites with lower GO content provided a slower release of 5-FU. Further analysis of kinetic model coefficients also suggested compatibility with zero-order kinetic model with the highest R^2 of 0.9750 and 0.9282 for GO/PU-1 and GO/PU-3 respectively (Table 5). Higher correlation with zero-order kinetic model indicates controlled release of 5-FU from the composites. In drug delivery systems, zero-order drug release kinetic enables the release of drug at a constant rate in a prolonged period of time. Limiting the initial burst release provides the maintenance of drug plasma concentration within the therapeutic window, which in turn minimize side effects and dose frequency. In addition, overall cumulative drug dosage is decreased in comparison with a drug release system exhibiting initial burst, leading to reduced risk of chronic toxicity. For these reasons, in case of drugs with short biological half-life and narrow therapeutic window such as 5-FU, maintaining zero-order drug release kinetics emerges as an advantageous outcome against clinical limitations.[67] The n values after fitting Korsmeyer−Peppas model were detected as 0.8526, 0.5754, and 0.4009 for GO/PU-1, GO/PU-3 and GO/PU-5 respectively. This indicated that GO/PU-1 and GO/PU-3 composites followed a non-Fickian transport mechanism, denoting that additional mechanisms were affecting release kinetics in addition to diffusion. Overall data exhibited the fact that GO addition resulted in faster release of 5-FU drug from the GO/PU matrix with a higher initial burst percentage. Possible explanation for this behavior is that agglomeration of the graphene oxide layers formed voids in the polymer matrix. In this context, graphene oxide might have acted as a filler leading to the reduction of tortuous path in polymer matrix, which in turn could have facilitated the release of 5-FU drug.[68]

The summary of previous studies investigating the drug release of various drugs from PU based carriers is presented in Table 6 in comparison with this study. Evaluated kinetic model studies mostly pointed out Higuchi and Korsmeyer−Peppas kinetic model as the best-fit models.

https://doi.org/10.1021/acsomega.4c02247
ACS Omega 2024, 9, 47395−47409

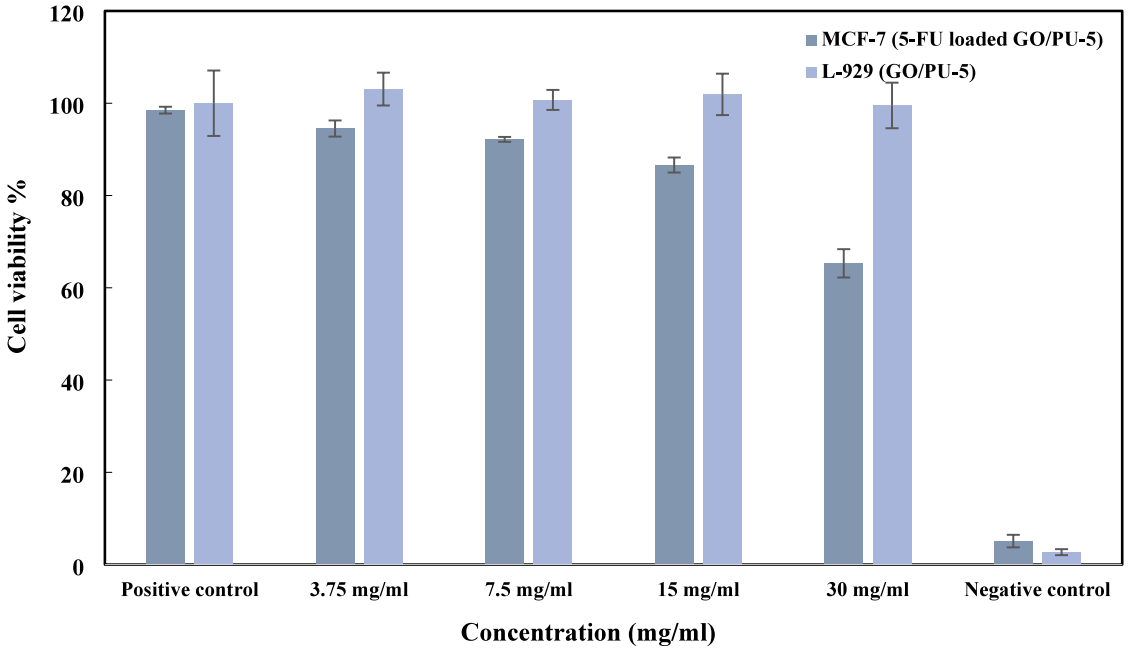

Figure 12. In vitro toxicity of 5-FU loaded GO/PU-5 against MCF-7 human breast cancer cells and blank GO/PU-5 against L-929 mouse fibroblast cells via the MTT assay test.

3.6. In Vitro Toxicity. In vitro cytotoxicity of 5-FU loaded and unloaded GO/PU films was investigated against human breast cancer cell line (MCF-7) and mouse fibroblast cell line (L-929) respectively via MTT assay test. GO/PU-5 and 5-FU incorporated GO/PU-5 composites were chosen for biological evaluation, as the highest drug release tendency was determined for this ratio from experimental design studies. Prior to the cytotoxicity test, GO/PU-5 films were subjected to extraction by placing them into Dulbecco's Modified Eagle Medium (DMEM) without serum with a concentration of 6 cm^2/ml at 37 °C ± 0.1 for 24 h. L-929 and MCF-7 cell lines were seeded onto a well plate at a concentration of 10^5 cell/ml, and film extracts were added afterward. Following the incubation for 24 h in a humidified environment with 5% CO_2 at 37 °C, the cell viability percentage was monitored via MTT assay by absorbance measurement at 570 nm for various mass concentrations of films. All measurements were replicated for 3 times. As observed from Figure 12, GO/PU-5 displayed a high cell viability of L-929 cells up to 30 mg/mL concentration, indicating an excellent biocompatibility. Meanwhile, the elimination of MCF-7 cancer cells was increased with increasing film concentration, after incubation with 5-FU loaded GO/PU-5 film extract solution. Minimum cell viability occurred at 30 mg/mL film concentration as 65.3 ± 3.1%. According to ISO 10993-5:2009 standard, cell viability below 70% threshold could be interpreted as cytotoxic activity of composite film was present.[72] Due to the fact that viability of L-929 cells for unloaded GO/PU-5 composite was at the highest, possible contribution of blank film to cytotoxic effect observed for loaded film could be eliminated and attributed to 5-FU drug only. The reduction in MCF-7 cell numbers confirmed the release of 5-FU from composite film during the extraction period, which led to approximately 35% cell death consequently.

4. CONCLUSIONS

In the current study, 5-FU incorporated graphene oxide/oil-based polyurethane composite films have been produced for the controlled delivery of 5-FU. The chemical and morphological structures of produced composites were examined via FTIR, TGA and SEM analysis measurements, confirming the successful polyurethane and composite production. In vitro designed experimental studies demonstrated that release percentage of 5-FU drug were enhanced at basic pH conditions (pH 10) and with higher GO contents. While continuous release of 5-FU drug was observed for all conditions in release kinetic studies, a higher correlation with the Higuchi kinetic model was detected at all pH values for maximum GO content, suggesting a release mechanism based on both drug dissolution and diffusion. Reducing the GO content resulted in compliance with the zero-order kinetic model at physiological pH, indicating an improving effect on controlled release by limiting the initial burst ratio. In vitro toxicity evaluation results confirmed the good biocompatibility of GO/PU composite film, whereas the 5-FU incorporated film displayed a cytotoxic effect against the MCF-7 breast cancer cell line, confirming the release of 5-FU from the film matrix. Overall data indicated a pH sensitive release mechanism of GO/PU composites, which could be tailored by altering selected experiment design factors, including GO and 5-FU amount.

■ ASSOCIATED CONTENT

Supporting Information

The Supporting Information is available free of charge at https://pubs.acs.org/doi/10.1021/acsomega.4c02247.

5-FU drug release profiles from GO/PU-5 composite at pH 1.2, 5.0, and 7.4 and 37 °C for various kinetic models; 5-FU drug release profiles from GO/PU-1 composite at pH 7.4 and 37 °C for various kinetic models; 5-FU drug release profiles from GO/PU-3

https://doi.org/10.1021/acsomega.4c02247
ACS Omega 2024, 9, 47395−47409

composite at pH 7.4 and 37 °C for various kinetic models (PDF)

AUTHOR INFORMATION

Corresponding Author

Ebru Kahraman − *Chemical Engineering Department, Istanbul Technical University, Istanbul 34469, Turkey;* orcid.org/0000-0002-9845-0979; Email: kahramaneb@itu.edu.tr

Authors

Tugba Hayri-Senel − *Chemical Engineering Department, Istanbul Technical University, Istanbul 34469, Turkey*

Gulhayat Nasun-Saygili − *Chemical Engineering Department, Istanbul Technical University, Istanbul 34469, Turkey*

Complete contact information is available at: https://pubs.acs.org/10.1021/acsomega.4c02247

Author Contributions

E.K.: Development or design of methodology; creation of models. Verification, whether as a part of the activity or separate, of the overall replication/reproducibility of results/experiments and other research outputs. Application of statistical, mathematical, computational, or other formal techniques to analyze or synthesize study data. Conducting a research and investigation process, specifically performing the experiments, or data/evidence collection. Provision of study materials, reagents, materials, patients, laboratory samples, instrumentation, computing resources, or other analysis tools. Preparation, creation and/or presentation of the published work, specifically writing the initial draft (including substantive translation). T.H.S.: Development or design of methodology; creation of models. Conducting a research and investigation process, specifically performing the experiments, or data/evidence collection. Provision of study materials, reagents, materials, patients, laboratory samples, instrumentation, computing resources, or other analysis tools. G.N.-S.: Development or design of methodology; creation of models. Provision of study materials, reagents, materials, patients, laboratory samples, instrumentation, computing resources, or other analysis tools. Those from the original research group, specifically critical review, commentary or revision−including preor postpublication stages. Oversight and leadership responsibility for the research activity planning and execution, including mentorship external to the core team.

Notes

The authors declare no competing financial interest.

ACKNOWLEDGMENTS

This study was supported by Istanbul Technical University BAP (grant-42197).

REFERENCES

(1) Sung, H.; Ferlay, J.; Siegel, R. L.; Laversanne, M.; Soerjomataram, I.; Jemal, A.; Bray, F. Global cancer statistics 2020: GLOBOCAN estimates of incidence and mortality worldwide for 36 cancers in 185 countries. *Ca - Cancer J. Clin.* **2021**, *71* (3), 209−249.

(2) Llamas-Ramos, I.; Alvarado-Omenat, J. J.; Rodrigo-Reguilón, M.; Llamas-Ramos, R. Quality of life and side effects management in cancer treatment—a cross sectional study. *Int. J. Environ. Res. Public Health.* **2023**, *20* (3), 1708.

(3) Muñoz, R.; Singh, D. P.; Kumar, R.; Matsuda, A. Graphene oxide for drug delivery and cancer therapy. In *Nanostructured Polymer Composites for Biomedical Applications*; Swain, S. K., Jawaid, M., Eds.; Elsevier Inc.: Netherlands, 2019; pp 447−488.

(4) Ghorai, T. K. Graphene oxide-based nanocomposites and biomedical applications. In *Functional Polysaccharides for Biomedical Applications*; Maiti, S., Jana, S., Eds.; Woodhead Publishing: United Kingdom, 2019; pp 305−328.

(5) Chng, E. L. K.; Pumera, M. The toxicity of graphene oxides: dependence on the oxidative methods used. *Chem.—Eur. J.* **2013**, *19* (25), 8227−8235.

(6) Li, C.; Li, F.; Wang, K.; Wang, Q.; Liu, H.; Sun, X.; Xie, D. Synthesis, characterizations, and release mechanisms of carboxymethyl chitosan-graphene oxide-gelatin composite hydrogel for controlled delivery of drug. *Inorg. Chem. Commun.* **2023**, *155*, 110965.

(7) Hasanin, M.; Taha, N. F.; Abdou, A. R.; Emara, L. H. Green decoration of graphene oxide nano sheets with gelatin and gum Arabic for targeted delivery of doxorubicin. *Biotechnol. Rep.* **2022**, *34*, e00722.

(8) Erol, Ü. H.; Güncüm, E.; Işıklan, N. Development of chitosan-graphene oxide blend nanoparticles for controlled flurbiprofen delivery. *Int. J. Biol. Macromol.* **2023**, *246*, 125627.

(9) Rajaei, M.; Rashedi, H.; Yazdian, F.; Navaei-Nigjeh, M.; Rahdar, A.; Díez-Pascual, A. M. Chitosan/agarose/graphene oxide nanohydrogel as drug delivery system of 5-fluorouracil in breast cancer therapy. *J. Drug Delivery Sci. Technol.* **2023**, *82*, 104307.

(10) Kafashan, A.; Joze-Majidi, H.; Babaei, A.; Shahrampour, D.; Arab-Bafrani, Z.; Arefkhani, M. Designing a nanohybrid complex based on graphene oxide for drug delivery purposes; investigating the intermediating capability of carbohydrate polymers. *Mater. Today Chem.* **2023**, *33*, 101751.

(11) Matiyani, M.; Rana, A.; Karki, N.; Garwal, K.; Pal, M.; Sahoo, N. G. Development of multi-functionalized graphene oxide based nanocarrier for the delivery of poorly water soluble anticancer drugs. *J. Drug Delivery Sci. Technol.* **2023**, *83*, 104412.

(12) Schifino, G.; Gasparini, C.; Drudi, S.; Giannelli, M.; Sotgiu, G.; Posati, T.; Zamboni, R.; Treossi, E.; Maccaferri, E.; Giorgini, L.; Mazzaro, R.; Morandi, V.; Palermo, V.; Bertoldo, M.; Aluigi, A. Keratin/polylactic acid/graphene oxide composite nanofibers for drug delivery. *Int. J. Pharm.* **2022**, *623*, 121888.

(13) Zhang, B.; Yan, Y.; Shen, Q.; Ma, D.; Huang, L.; Cai, X.; Tan, S. A colon targeted drug delivery system based on alginate modificated graphene oxide for colorectal liver metastasis. *Mater. Sci. Eng. C* **2017**, *79*, 185−190.

(14) Rao, Z.; Ge, H.; Liu, L.; Zhu, C.; Min, L.; Liu, M.; Fan, L.; Li, D. Carboxymethyl cellulose modified graphene oxide as pH-sensitive drug delivery system. *Int. J. Biol. Macromol.* **2018**, *107*, 1184−1192.

(15) Pooresmaeil, M.; Namazi, H. *β*-Cyclodextrin grafted magnetic graphene oxide applicable as cancer drug delivery agent: synthesis and characterization. *Mater. Chem. Phys.* **2018**, *218*, 62−69.

(16) Hussien, N. A.; Işıklan, N.; Türk, M. Pectin-conjugated magnetic graphene oxide nanohybrid as a novel drug carrier for paclitaxel delivery. *Artif. Cells, Nanomed., Biotechnol.* **2018**, *46*, 264−273.

(17) Alibolandi, M.; Mohammadi, M.; Taghdisi, S. M.; Ramezani, M.; Abnous, K. Fabrication of aptamer decorated dextran coated nano-graphene oxide for targeted drug delivery. *Carbohydr. Polym.* **2017**, *155*, 218−229.

(18) Patel, D. K.; Senapati, S.; Mourya, P.; Singh, M. M.; Aswal, V. K.; Ray, B.; Maiti, P. Functionalized graphene tagged polyurethanes for corrosion inhibitor and sustained drug delivery. *ACS Biomater. Sci. Eng.* **2017**, *3* (12), 3351−3363.

(19) Das, A.; Mahanwar, P. A brief discussion on advances in polyurethane applications. *Adv. Ind. Eng. Polym. Res.* **2020**, *3* (3), 93−101.

(20) Araujo, T. R.; Bresolin, D.; de Oliveira, D.; Sayer, C.; de Araujo, P. H. H.; de Oliveira, J. V. Conventional lignin functionalization for polyurethane applications and a future vision in the use of enzymes as an alternative method. *Eur. Polym. J.* **2023**, *188*, 111934.

(21) Cui, M.; Chai, Z.; Lu, Y.; Zhu, J.; Chen, J. Developments of polyurethane in biomedical applications: a review. *Resour. Chem. Mater.* **2023**, *2* (4), 262−276.

(22) Park, J.; Lee, M. J.; Ahn, G. Y.; Yun, T. H.; Choi, I.; Lee, E. S.; Lee, H.; Choi, S. W. Synthesis and characterizations of biodegradable polyurethane microspheres with dexamethasone for drug delivery. *Macromol. Res.* **2019**, *27*, 839−842.
(23) Babanejad, N.; Nabid, M. R.; Farhadian, A.; Dorkoosh, F.; Zarrintaj, P.; Saeb, M. R.; Mozafari, M. Sustained delivery of olanzapine from sunflower oil based polyol urethane nanoparticles synthesised through a cyclic carbonate ring opening reaction. *IET Nanobiotechnol.* **2019**, *13* (7), 703−711.
(24) Sagitha, P.; Reshmi, C. R.; Sundaran, S. P.; Binoy, A.; Mishra, N.; Sujith, A. In-vitro evaluation on drug release kinetics and antibacterial activity of dextran modified polyurethane fibrous membrane. *Int. J. Biol. Macromol.* **2019**, *126*, 717−730.
(25) Javaid, M. A.; Jabeen, S.; Arshad, N.; Zia, K. M.; Hussain, M. T.; Bhatti, I. A.; Iqbal, A.; Ahmad, S.; Ullah, I. Development of amylopectin based polyurethanes for sustained drug release studies. *Int. J. Biol. Macromol.* **2023**, *244*, 125224.
(26) Shoaib, M.; Bahadur, A.; Iqbal, S.; Rahman, M. S. U.; Ahmed, S.; Shabir, G.; Javaid, M. A. Relationship of hard segment concentration in polyurethane-urea elastomers with mechanical, thermal and drug release properties. *J. Drug Delivery Sci. Technol.* **2017**, *37*, 88−96.
(27) Anghel, N.; Dinu, V. M.; Verestiuc, L.; Spiridon, I. A. Transcutaneous drug delivery systems based on collagen/polyurethane composites reinforced with cellulose. *Polymers.* **2021**, *13* (11), 1845.
(28) Tao, W.; Wang, J.; Zhou, Y.; Liu, Z.; Chen, H.; Zhao, Z.; Yan, H.; Liao, X. Acid/reduction dual-sensitive amphiphilic graft polyurethane with folic acid and detachable poly(ethylene glycol) as anticancer drug delivery carrier. *Colloids Surf., B* **2023**, *222*, 113084.
(29) Kamaci, M. Polyurethane-based hydrogels for controlled drug delivery applications. *Eur. Polym. J.* **2020**, *123*, 109444.
(30) Wienen, D.; Gries, T.; Cooper, S. L.; Heath, D. E. An overview of polyurethane biomaterials and their use in drug delivery. *J. Controlled Release* **2023**, *363*, 376−388.
(31) Zhang, S.; Chu, F.; Zhou, Y.; Xu, Z.; Jiang, X.; Luo, X.; Yuan, G.; Hu, Y.; Hu, W. High-performance flexible polyurethane from renewable castor oil: preparation, properties and mechanism. *Composites, Part A* **2022**, *159*, 107034.
(32) Kaikade, D. S.; Sabnis, A. S. Polyurethane foams from vegetable oil-based polyols: a review. *Polym. Bull.* **2023**, *80*, 2239−2261.
(33) Asare, M. A.; Kote, P.; Chaudhary, S.; de Souza, F. M.; Gupta, R. K. Sunflower oil as a renewable resource for polyurethane foams: effects of flame-retardants. *Polymers.* **2022**, *14* (23), 5282.
(34) Chan, Y. Y.; Ma, C.; Zhou, F.; Hu, Y.; Schartel, B. Flame retardant flexible polyurethane foams based on phosphorous soybean-oil polyol and expandable graphite. *Polym. Degrad. Stab.* **2021**, *191*, 109656.
(35) Petrović, Z. S.; Yang, L.; Zlatanić, A.; Zhang, W.; Javni, I. Network structure and properties of polyurethanes from soybean oil. *J. Appl. Polym. Sci.* **2007**, *105* (5), 2717.
(36) Tanaka, R.; Hirose, S.; Hatakeyama, H. Preparation and characterization of polyurethane foams using a palm oil-based polyol. *Bioresour. Technol.* **2008**, *99* (9), 3810−3816.
(37) Polaczek, K.; Kurańska, M.; Auguścik-Królikowska, M.; Prociak, A.; Ryszkowska, J. Open-cell polyurethane foams of very low density modified with various palm oil-based bio-polyols in accordance with cleaner production. *J. Cleaner Prod.* **2021**, *290*, 125875.
(38) Boddu, A.; Obireddy, S. R.; Subbarao, S. M. C.; Rao, K. M.; Venkata, K. R. K. S. Encapsulation of 5-fluorouracil treated reduced graphene oxide in sodium alginate matrix for controlled and ph-responsive drug delivery. *ChemistrySelect.* **2021**, *6*, 6533−6540.
(39) Dongsar, T. T.; Dongsar, T. S.; Gupta, N.; Almalki, W. H.; Sahebkar, A.; Kesharwani, P. Emerging potential of 5-Fluorouracil-loaded chitosan nanoparticles in cancer therapy. *J. Drug Delivery Sci. Technol.* **2023**, *82*, 104371.
(40) Longley, D. B.; Harkin, D. P.; Johnston, P. G. 5-fluorouracil: mechanisms of action and clinical strategies. *Nat. Rev. Cancer.* **2003**, *3*, 330−338.
(41) Gazestani, A. M.; Khoeia, S.; Khoee, S.; Minaei, S. E.; Motevalian, M. In vivo evaluation of the combination effect of near-infrared laser and 5-fluorouracil-loaded PLGA-coated magnetite nanographene oxide. *Artif. Cells, Nanomed., Biotechnol.* **2018**, *46* (2), 25−33.
(42) Kahraman, E.; Erdol Aydin, N.; Nasun-Saygili, G. Optimization of 5-FU adsorption on gelatin incorporated graphene oxide nanocarrier and application for antitumor activity. *J. Drug Delivery Sci. Technol.* **2023**, *80*, 104153.
(43) Hayri-Senel, T.; Yazgan-Birgi, P.; Bildik, F.; Erciyes, A. T. The use of poly(styrene-co-chloromethyl styrene) in the modification of triglyceride oils. *J. Coat. Technol. Res.* **2022**, *19*, 1583−1593.
(44) Gurgel, D.; Bresolin, D.; Sayer, C.; Filho, L. C.; Araújo, P. H. H. Flexible polyurethane foams produced from industrial residues and castor oil. *Ind. Crops Prod.* **2021**, *164*, 113377.
(45) Karak, N. Vegetable oils and their derivatives. In *Vegetable Oil-Based Polymers Properties, Processing and Applications*; Woodhead Publishing: United Kingdom, 2012; pp 54−95.
(46) Prieto, S. F.; Franco, J. M.; Garcia, I. M.; Raghunanan, L. C.; Frankenbach, G. M. Adhesives derived from castor oil. European Patent EP3453729A1, 2018.
(47) Noyes, A. A.; Whitney, W. R. The rate of solution of solid substances in their own solutions. *J. Am. Chem. Soc.* **1897**, *19* (12), 930−934.
(48) Korsmeyer, R. W.; Gurny, R.; Doelker, E.; Buri, P.; Peppas, N. A. Mechanisms of solute release from porous hydrophilic polymers. *Int. J. Pharm.* **1983**, *15* (1), 25−35.
(49) Higuchi, T. Rate of release of medicaments from ointment bases containing drugs in suspension. *J. Pharm. Sci.* **1961**, *50* (10), 874−875.
(50) Hixson, A. W.; Crowell, J. H. Dependence of reaction velocity upon surface and agitation. *Ind. Eng. Chem.* **1931**, *23* (8), 923−931.
(51) Mathematical models of drug release. In *Strategies to Modify the Drug Release from Pharmaceutical Systems*; Bruschi, M. L., Ed.; Woodhead Publishing: United Kingdom, 2015; pp 63−86.
(52) Peng, S. J.; Jin, Y.; Cheng, X. F.; Sun, T. B.; Qi, R.; Fan, B. Z. A new method to synthesize high solid content waterborne polyurethanes by strict control of bimodal particle size distribution. *Prog. Org. Coat.* **2015**, *86*, 1−10.
(53) Dias, R. C. M.; Goes, A. M.; Serakides, R.; Ayres, E.; Orefice, R. L. Porous biodegradable polyurethane nanocomposites: preparation, characterization, and biocompatibility tests. *Mater. Res.* **2010**, *13* (2), 211−218.
(54) Liu, H.; Huang, W.; Yang, X.; Dai, K.; Zheng, G.; Liu, C.; Shen, C.; Yan, X.; Guo, J.; Guo, Z. Organic vapor sensing behaviors of conductive thermoplastic polyurethane-graphene nanocomposites. *J. Mater. Chem. C* **2016**, *4* (20), 4459−4469.
(55) Ahmed, N.; Atif, M.; Ahmed, N.; Iftikhar, F.; Nauman, S.; Niaz, B. Polyurethane polystyrene based smart interpenetrating network with quick shape recovery through thermal actuation. *Polym. Polym. Compos* **2022**, *30*, 096739112210768.
(56) Tan, R. Y. H.; Lee, C. S.; Pichika, M. R.; Cheng, S. F.; Lam, K. Y. pH responsive polyurethane for the advancement of biomedical and drug delivery. *Polymers.* **2022**, *14* (9), 1672.
(57) Wielińska, J.; Nowacki, A.; Liberek, B. 5-fluorouracil-complete insight into its neutral and ionised forms. *Molecules.* **2019**, *24* (20), 3683.
(58) Mioduszewska, K.; Dołżonek, J.; Wyrzykowski, D.; Kubik, Ł.; Wiczling, P.; Sikorska, C.; Toński, M.; Kaczyński, Z.; Stepnowski, P.; Białk-Bielińska, A. Overview of experimental and computational methods for the determination of the pKa values of 5-fluorouracil, cyclophosphamide, ifosfamide, imatinib and methotrexate. *TrAC, Trends Anal. Chem.* **2017**, *97*, 283−296.
(59) Simeonova, M.; Velichkova, R.; Ivanova, G.; Enchev, V.; Abrahams, I. Poly(butylcyanoacrylate) nanoparticles for topical delivery of 5-fluorouracil. *Int. J. Pharm.* **2003**, *263* (1−2), 133−140.
(60) Obireddy, S. R.; Lai, W. F. Multi-component hydrogel beads incorporated with reduced graphene oxide for pH-responsive and

https://doi.org/10.1021/acsomega.4c02247
ACS Omega 2024, 9, 47395−47409

controlled co-delivery of multiple agents. *Pharmaceutics.* **2021**, *13*, 313.
(61) Li, W.; Liu, D.; Zhang, H.; Correia, A.; Mäkilä, E.; Salonen, J.; Hirvonen, J.; Santos, H. A. Microfluidic assembly of a nano-in-micro dual drug delivery platform composed of halloysite nanotubes and a pH-responsive polymer for colon cancer therapy. *Acta Biomater.* **2017**, *48*, 238−246.
(62) Sun, Q.; Wang, X.; Cui, C.; Li, J.; Wang, Y. Doxorubicin and anti-VEGF siRNA co-delivery via nano-graphene oxide for enhanced cancer therapy in vitro and in vivo. *Int. J. Nanomed.* **2018**, *13*, 3713−3728.
(63) Tatiparti, K.; Rauf, M. A.; Sau, S.; Iyer, A. K. Carbonic anhydrase-IX guided albumin nanoparticles for hypoxia-mediated triple-negative breast cancer cell killing and imaging of patient-derived tumor. *Molecules.* **2020**, *25* (10), 2362.
(64) Kar, S.; Kundu, B.; Reis, R. L.; Sarkar, R.; Nandy, P.; Basu, R.; Das, S. Curcumin ameliorates the targeted delivery of methotrexate intercalated montmorillonite clay to cancer cells. *Eur. J. Pharm. Sci.* **2019**, *135*, 91−102.
(65) Vieira, I. R. S.; Miranda, G. D. S.; Ricci-Júnior, E.; Delpech, M. C. Waterborne poly(urethane-urea)s films as a sustained release system for ketoconazole. *E-Polym.* **2019**, *19* (1), 168−180.
(66) Wang, L.; Gao, J.; An, Z.; Zhao, X.; Yao, H.; Zhang, M.; Tian, Q.; Zhai, X.; Liu, Y. Polymer microsphere for water-soluble drug delivery via carbon dot-stabilizing W/O emulsion. *J. Mater. Sci.* **2019**, *54*, 5160−5175.
(67) Laracuente, M. L.; Yu, M. H.; McHugh, K. J. Zero-order drug delivery: state of the art and future prospects. *J. Controlled Release* **2020**, *327*, 834−856.
(68) Patel, D. K.; Singh, R. K.; Singh, S. K.; Aswal, V. K.; Rana, D.; Ray, B.; Maiti, P. Graphene as a chain extender of polyurethanes for biomedical applications. *RSC Adv.* **2016**, *6* (63), 58628−58640.
(69) Avelino, F.; Miranda, I. P.; Moreira, T. D.; Becker, H.; Romero, F. B.; Taniguchi, C. A. K.; Mazzetto, S. E.; Filho, M. S. M. S. The influence of the structural features of lignin-based polyurethane coatings on ammonium sulfate release: kinetics and thermodynamics of the process. *J. Coat. Technol. Res.* **2019**, *16*, 449−463.
(70) Verstraete, G.; Vandenbussche, L.; Kasmi, S.; Nuhn, L.; Brouckaert, D.; Van Renterghem, J.; Grymonpré, W.; Vanhoorne, V.; Coenye, T.; De Geest, B. G.; De Beer, T.; Remon, J. P.; Vervaet, C. Thermoplastic polyurethane-based intravaginal rings for prophylaxis and treatment of (recurrent) bacterial vaginosis. *Int. J. Pharm.* **2017**, *529* (1−2), 218−226.
(71) Xu, J.; Hao, T.; Liu, C.; Bi, J.; Sun, J.; Wen, Z.; Hou, Z.; Wei, J. pH-Responsive and degradable polyurethane film with good tensile properties for drug delivery *in vitro*. *Mater. Today Commun.* **2021**, *29*, 102969.
(72) Nedeljkovic, I.; Doulabi, B. Z.; Abdelaziz, M.; Feilzer, A. J.; Exterkate, R. A. M.; Szafert, S.; Gulia, N.; Krejci, I.; Kleverlaan, C. J. Cytotoxicity and anti-biofilm properties of novel hybrid-glass-based caries infiltrant. *Dent. Mater.* **2022**, *38* (12), 2052−2061.

https://doi.org/10.1021/acsomega.4c02247
ACS Omega 2024, 9, 47395−47409